인체탐상용 초소형 와전류 센서 메커니즘 개발
Development of Eddy Current Sensor Mechanism for the Anthroposcopy

*#김철웅[1], 서용범[2], 송성철[2], 김희성[2]
*#C. W. Kim(woong25@korea.ac.kr)[1] , Y. B. Seo[2] , S. C. Song[2] and H. S. Kim[2]
[1]고려대학교/(주)트리플씨메디칼, [2]케이엔디티앤아이(주)

Key words : Eddy Current, Sensor Mechanism, Magnetic Susceptibility, Electrical Conductivity

---

1. Introduction

Shielding in magnetic field is more difficult than in electric field. So, it can be said that magnetic field influences the biocompatibility more than electric field. In order to prevent distortions in the image or magnetic field by the micro-pin after permanent transplant of an anastomotic ring during free flap or plastic reconstruction, the current density, magnetic susceptibility, and electrical conductivity of Ti-6Al-4V must be evaluated. This study simulated the following: 1) calculation of the current density created by micro-pin when radiated with magnetic field of 1T~4T(Tesla) 2) evaluation of electrical conductivity of the current density of the micro-pin. 3) verification of magnetic susceptibility with respect to the relative position between the micro-pins.

2. Analysis of 3-dimensional Magnetic Field with Respect to Biot-Savart's Law

The result of Finite Element Model (FEM) can be highly trusted when it contains finite plane as in electrical instruments. However, the evaluative analysis is rather vague for magnetic fields, thus limits 3-dimensional region segmentation. Consequently, it is more accurate to apply Biot-Savart's law if there is no dielectric substance. In this study, human tissue model was hypothesized to be a magnetic cube cell, modeled through Impedance Network, and analyzed after converting the Maxwell equation to Circuit Eq. Impedance method is highly effect for finding the inner current density or induced electric field if the frequency is low. When human tissue is exposed to a time-variant magnetic field, the human body becomes non-assimilative, hence, a critical factor that could influence the magnetic field. The eddy current can be calculated by forming an electrical network from the complex conductivity $\sigma + J\omega\epsilon$ of the tissue. $\overrightarrow{dB}$ is the magnetic field of point P that is r away from $i\overrightarrow{dl}$ and is defined by Eq. (1). The magnetic field of the finite straight wire $i\overrightarrow{\Delta l}$ is defined by Eq. (3), integrated by Eq. (2).

$$\overrightarrow{dB} = \frac{\mu_0}{4\pi}\frac{i\overrightarrow{dl}\times\vec{r}}{r^3} \tag{1}$$

$$\overrightarrow{dB} = \frac{\mu_0 i}{4\pi}\frac{\rho\, dz\, \overrightarrow{u_\phi}}{\left(\rho^2+z^2\right)^{3/2}} \tag{2}$$

$$B = \frac{\mu_0 i\, \overrightarrow{u_\phi}}{4\pi\rho}\left(\sin\alpha_1 + \sin\alpha_2\right) \tag{3}$$

From a particular point of a space to an equation of 3-dimensional A.C. magnetic field vector B, the phase difference in each exes is considered and is defined as Eq. (4) by assuming a single frequency.

$$\begin{aligned} B(t) = {} & \sqrt{2}\,B_x \sin(\omega t)\, i + \sqrt{2}\,B_y \sin(\omega t+\alpha)\, j \\ & + \sqrt{2}\,B_z \sin(\omega t+\beta)\, k \end{aligned} \tag{4}$$

In 3-dimensional magnetic field, when $\alpha = \beta = 0$, it becomes a straight line. Under other conditions, it becomes an oval or a circle. The direction vector of magnetic vector B is given in Eq. (5).

$$e\left(e_x, e_y, e_z\right) = e\left\{B_x \sin(\omega t),\ B_y \sin(\omega t+\alpha),\ B_z \sin(\omega t+\beta)\right\} \tag{5}$$

The virtual value B_{rms} of magnetic field B is defined as Eq. (6) by the average of one endogenous periodicity $T(=1/f=2\pi/\omega)$ of B.

$$\begin{aligned} B_s &= \sqrt{\frac{1}{T}\int_{-T/2}^{T/2} B \cdot B dt} = \sqrt{\frac{\omega}{2}\pi\int_{-\pi/\omega}^{\pi/\omega} B \cdot B dt} \\ &= \sqrt{\omega\pi\int_{-\pi/\omega}^{\pi/\omega}\left\{\begin{array}{l} B_x^2 \sin^2\omega t + B_y^2 \sin^2(\omega t+\alpha) \\ + B_z^2 \sin^2(\omega t+\beta) \end{array}\right\} dt} \end{aligned} \tag{6}$$

The virtual value B_{rms} of magnetic field B calculated in Eq. (6) is described in Eq. (7).

$$B_s = \sqrt{B_x^2 + B_y^2 + B_z^2} \tag{7}$$

In IEEE Standard, the sum of squared virtual value of each axial magnetic field elements is square rooted. The value is then defined as resultant magnetic field and applied in Eq. (7) in the same manner.

3. Analysis of Magnetic Field and Establishing an MRI Machine System Through Finite Element Model

There are three kinds of magnets used for Magnetic Resonance (MR): permanent magnet, electromagnet, and super conductive magnet. MRI provides a high resolution image so that one can observe fine tissue inside a human body. In most MRI's, superconductive magnets are used. NbTi(Niobium-Titanium) is used for superconductors that require high uniformity, reliability, and safety. An MRI that uses superconductor needs to be at absolute temperature of 4.2K (-268.8℃) as Helium and Nitrogen must be maintained in liquid state. Though an MRI that uses superconductor provides high resolution image, it requires a lot of maintenance cost. Consequently, MRI that employes permanent magnet is the most widely accepted diagnostic instrument. Hence, this research only evaluated an MRI that uses permanent magnets. As stated in systems of coordinates Fig. 1 and Fig 2, MRI that uses permanent magnets is a y-axis symmetrical model, half-modeling technique was applied for optimization and analysis process. The corresponding rough plan and design domain are represented in Fig. 2. For optimization process, the pole and yolk parts were each defined as design domain I and II.

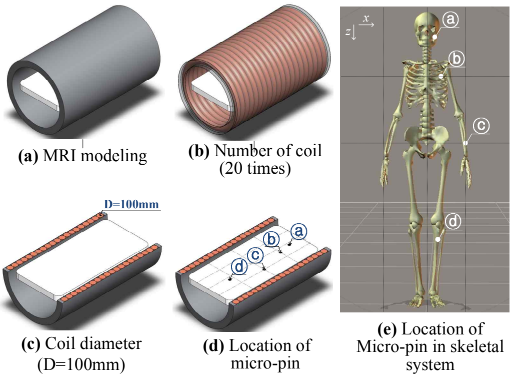

(a) MRI modeling

(b) Number of coil (20 times)

(c) Coil diameter (D=100mm)

(d) Location of micro-pin

(e) Location of Micro-pin in skeletal system

Fig. 1 Built-up of Magnetic Resonance Image (MRI) machine and location of anastomotic micro-pin in skeletal system

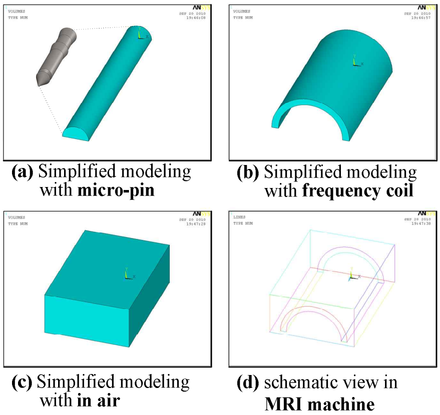

(a) Simplified modeling with **micro-pin**

(b) Simplified modeling with **frequency coil**

(c) Simplified modeling with **in air**

(d) schematic view in **MRI machine**

(i) Simplified modeling with modeling elements

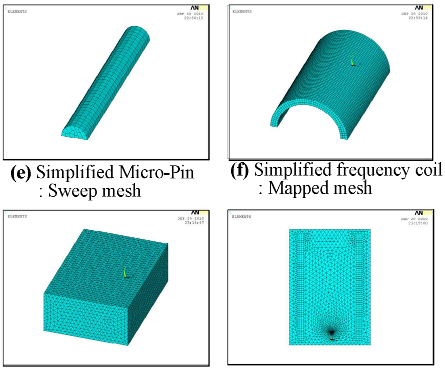

(e) Simplified Micro-Pin : Sweep mesh

(f) Simplified frequency coil : Mapped mesh

(g) Air (adjacent atmosphere) : Free mesh

(h) Geometries of mesh with micro-pin

(ii) Meshing with each modeling elements

Fig. 2 Simplified modeling and meshing in micro-pin, frequency coil, in air, and MRI machine

4. Conclusions

The material of the pin is Ti-6Al-4V which may be displaced towards the coil and cause heat in human body depending on the magnetic and electric densities of an MRI system. Therefore, the actual magnetic and electric densities loaded on a pin by an MRI were evaluated. 1T/one-pin showed the highest magnetic density on hand part, and 1T/two-pin showed the highest magnetic density on chest part. However, in 2T, both one-pin and two-pin showed the highest magnetic density on head part.

Acknowledgment

This study was funded by the Medical Health Research Development Project (Futuristic Medical Appliances Development Project) of the Ministry of Health and Welfare (A092140).